COMPDYN 2015
5th ECCOMAS Thematic Conference on
Computational Methods in Structural Dynamics and Earthquake Engineering
M. Papadrakakis, V. Papadopoulos, V. Plevris (eds.)
Crete Island, Greece, 25–27 May 2015

INVESTIGATION OF NOVEL ANCHORING DEVICES FOR OPEN HOOP CFRP STRIPS BONDED ON R/C ELEMENTS UNDER MONOTONIC AND CYCLIC LOADING-UNLOADING CONDITIONS

Konstantinos B. Katakalos[2] and George C. Manos[1]

[1,2] Aristotle University of Thessaloniki
School of Engineering, Egnatia street, University Campus, Thessaloniki, Greece
e-mail: kkatakal@auth.gr, gcmanos@civil.auth.gr

Keywords: Strengthening schemes, R/C elements and CFRP sheets, Novel anchoring devices, load-unload cyclic sequence.

Abstract. *Results obtained from research conducted in the framework of an initiative introduced by the Hellenic Earthquake Planning and Protection Organization aiming to support relevant provisions of the Greek Code for the repair and strengthening of R/C structures are presented and discussed. When trying to utilize fiber polymer sheets, as external reinforcement attached on R/C elements, their potential of high tensile strength is prevented by the FRP sheets' debonding mode of failure thus limiting the exploitation of the material. In order to confront this limitation the effectiveness of two novel types of anchoring devices that can be incorporated together with such FRP strips was studied. For this purpose special unit beam concrete specimens were fabricated and were used to attach the open hoop carbon strips (CFRP). The novel loading arrangement developed at Laboratory of Strength of Materials and Structures was utilized to apply the necessary forces to these unit beam specimens together with instrumentation capable of capturing the behavior of these specimens up to failure. Studying in this way the transfer of forces from the open hoop FRP strips it could be demonstrated that when this type of retrofitting was accompanied with a properly designed anchoring device, a significant increase in the bearing capacity of the tested specimens was observed. The present investigation incorporates also the influence of number of cycles, in a loading-unloading way, on the overall behavior of the strengthening scheme, in terms of ultimate strength and observed mode of failure. Finally, this paper includes the most important findings of a supplementary numerical investigation, using the FEA software ABAQUS, aimed to study the behaviour of the novel anchoring device which is patented in Europe under the patent number WO2011073696.*

1 INTRODUCTION

Many reinforced concrete (R/C) structural members need strengthening either because they were built according to old code provisions and do not meet the current design requirements, or because they are damaged after extreme events such as a strong earthquake sequence and they are in need of repair and strengthening. [1,2] When such a strengthening scheme uses externally bonded FRP layers one of the basic problems is the effectiveness of the anchorage of these polymer sheets to the concrete parts. This is necessary, in order to transfer successfully the desired level of tensile forces that develop on these layers and to exploit their high tensile capacity. Thus the satisfactory behavior of such an anchorage scheme, without premature failure, becomes critical in order to utilize successfully the high levels of tensile forces that these FRP layers can withstand and thus meet the strengthening design requirements for the structural members under consideration.

There is a real necessity to develop reliable anchoring details that can accompany repair and strengthening schemes of Reinforced Concrete elements employing FRP layers in such a way that the FRP parts together with their anchoring detail can provide a feasible and safe solution for such an application.

When fiber reinforced polymer sheets are bonded to the face of an R/C member with the use of a structural epoxy resin, the most common type of failure is the debonding of the FRP sheets from the structural member. Numerous researchers [1-6] have conducted experiments to study this debonding type of failure (figure 1) and to investigate means for improvement. It was shown that the desired capacity of such a R/C member strengthened with the use of FRP's could be reached easier when this debonding type of failure of the FRP sheets is delayed. It was also demonstrated that the surface preparation can be of importance for delaying this debonding type of failure. Apart from the good bonding an alternative way is to use appropriate anchoring devices. It was also shown [7-11] that utilizing mechanical anchors one can rely less on the bond which is provided to the FRP-concrete interface by the use commercially available epoxy resins.

The work reported here is an extension of the research performed by Manos and Katakalos [16] on effective anchoring devices of externally bonded FRP strips. Such devices can uphold the premature FRP strip debonding mode of failure and instead direct the mode of failure to the fracture of the FRP strip, thus resulting in a substantial increase of the ultimate bearing capacity of the strengthening scheme.

2 NOVEL ANCHORING SCHEMES UNDER MONOTONIC LOADINGS NUMRICAL AND EXPERIMENTAL INVESTIGATIONS

2.1 Experimental Setup

The present research aims to investigate the effectiveness of a specific FRP anchoring device (SWFX) combined with a typical FRP strip, by applying them to a number of small concrete prismatic specimens, which can house such strengthening systems with sufficient width and length. Totally 12 specimens were investigated utilizing the novel experimental setup developed on the Laboratory of Strength of Materials and Structures (LSMS) [7, 16] which is presented in figure 1. The details of all specimens are presented in the following Table 1.

Two specimens were utilized as reference specimens having the CFRP strips fully wrapped around the concrete T-section prisms, as depicted in figure1. (Ref-1 and Ref-2) Three speci-

mens were utilized to investigate the behavior of the FRP anchoring scheme it self. (SWFX-1 to SWFX-3) Three specimens were tested having one layer of CFRP strip combined with one anchor; whereas four last specimens were investigated utilizing one layer of CFRP strip combined with two anchors. The materials were provided by SIKA Hellas, which is greatly acknowledged.

All concrete prisms were fabricated using the same concrete mix and the same internal reinforcement, which was used to prohibit any accidental failure. The measured cylinder strength of the concrete was equal to 22 MPa.

Table 1. Details of experimental investigation

Specimen's name	CFRP strip	Anchoring Scheme	No. of tests	Remarks
Ref	1 CFRP strip	No	2	Full Wrapped
SW600C/2	1 CFRP strip	2 X Anchors	4	System Lay Up: Anchor Spread / Fabric / Anchor Spread
SW600C/1	1 CFRP strip	1 X Anchor	3	System Lay Up: Anchor Spread / Fabric
SWFX	No strip	ONLY Anchor	3	Full Wrapping

The main goal of the experimental study is to investigate the combined behavior of the strengthening scheme (anchor + CFRP strip) and to demonstrate any limitations that may arise by the use of such anchoring schemes. For this specific investigation the experimental setup developed in the Laboratory of Strength of Materials and Structures of A.U.Th. (fig. 1) was utilized. [1, 7, 16]

The loading arrangement is also depicted in figure 1, whereby the tensile force is directly applied in the axis of symmetry at the concrete prism; two sides of the FRP strip are bonded in a symmetric way on the top and bottom side of the concrete prism, as shown in this figure.

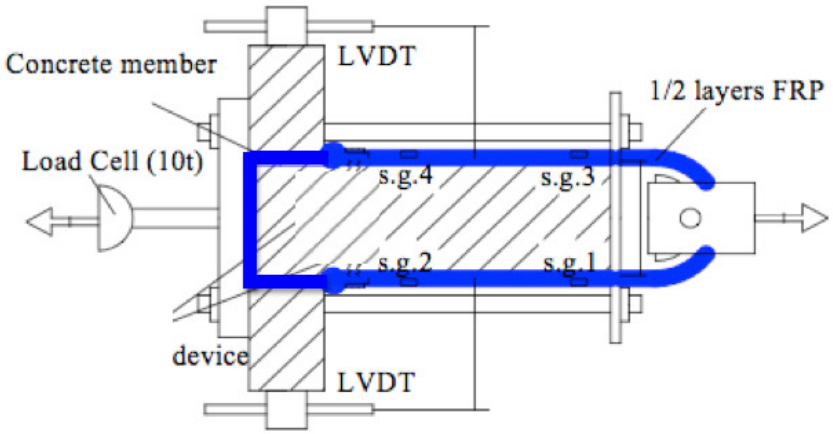

Figure 1. Novel experimental setup developped at LSMS premises [7].

Despite the symmetry of this test set-up, instrumentation was provided that is able to record symmetric as well as asymmetric response of the specimen, especially during the initiation and propagation of the debonding process. During testing, the applied load is measured together with the longitudinal (axial) strains at two different locations of the external surface of the FRP strip, as indicated in figure 1. (s.g.1 and s.g.3) The strains are measured in order to acquire an indication of the developed stresses locally at these specific locations.

The tested specimens with their details are listed in table 1 together with their reference names.

2.2 Experimental results and discussion – monotonic conditions

The summary of the experimental results is listed in Table 2. In this table, the observed failure mechanism is listed together with the corresponding value of the ultimate measured load at each CFRP strip. Moreover, the average maximum strain values measured by the strain gauges at locations 1 and 3 on the CFRP strip surface are also presented.

Table 2. Summary of the obtained results

Specimen's name	Load at each FRP strip (kN)	Average Load (kN)	Average strain from both sides	Average Strain (mm/mm)	Mode of failure
Ref-1	49.33	42.81	0.0066	0.0058	Fracture of FRP strip
Ref-2	36.30		0.0051		Fracture of FRP strip
SW600C/2 -1	39.73	43.06	0.0052	0.0053	Fracture of FRP strip
SW600C/2 -2	48.59		0.0064		Fracture of FRP strip
SW600C/2 -3	30.93		0.0042		Fracture of FRP strip first a width of 8mm
SW600C/2 -4	52.99		0.0053		Fracture of FRP strip
SW600C/1 -1	30.44	33.06	0.0039	0.0042	Fracture of anchor at upper corner
SW600C/1 -2	34.38		0.0044		Delamination of FRP strips form anchor
SW600C/1 -3	34.36		0.0044		Fracture of anchor at upper corner
SWFX -1	34.54	34.89	-		Fracture of anchor
SWFX -2	36.29		-		Fracture of anchor
SWFX -3	33.85		-		Fracture of anchor

CFRP strips of specimens Ref-1 and Ref-2 were fully wrapped around the concrete prisms and are utilized as reference specimens. The average ultimate load was recorded equal to 42.81kN. The mode of failure for both reference specimens was observed at the fracture of the strips. The mode of failure for all specimens is presented in figures 2a to 2e. The performance of the FRP anchoring scheme was separately investigated before its application with CFRP strips. Specimens SWFX-1 to SWFX-3 were tested for this purpose monotonically to failure. The average ultimate load for these three specimens was equal to 34.89kN. The mode of failure was observed at the fracture of the anchoring scheme. (see figure 2d and figure 2e)

The anchoring scheme together with one layer of CFRP strip was applied to strengthen specimens SW600C/1-1 to SW600C/1-3. The average load for all three specimens was recorded equal to 33.06kN, whereas the mode of failure was observed to the fracture of the

Figure 2a. Ref-1 and Ref-2

Figure 2b. SW600C/2-2

Figure 2c. SW600C/1 -1

Figure 2c. SW600C/1 -2

Figure 2d. SWFX -1

Figure 2e. SWFX -2

anchoring scheme. As observed both SW600C/1 and SWFX exhibit similar average ultimate load and similar mode of failure. The premature failure of the anchor, before the fracture of the strip results in decreasing the exploitation of CFRP strips. The fact that the ultimate strength of both SW600C/1 and SWFX is similar, enhance the validity of the experimental investigation.

In order to avoid the premature failure of the anchoring scheme, specimens SW600C/2 were fabricated combining 2 anchors with one CFRP strip. The average load for the three specimens is equal to 43.06kN whereas the mode of failure was observed at the fracture of the CFRP strip. Following the previous rational when applying two anchors the CFRP strip is fully exploited since the mode of failure is located at the fracture of the strip itself.

The measured strains are also demonstrating the same observation. More specifically the average strain of specimens SW600C/2 is equal to 0.0053 (mm/mm) very similar with the measured strains of specimens ref-1 and ref-2. (0.0058 mm/mm) By comparing the average strains of SW600C/1 specimens with SW600C/2 specimens it could be said that the exploitation of the strips increased almost 30%. Summarizing, the use of two anchors combined with one CFRP strip (width=100mm) ensures the full nominal exploitation of the strip, drives the mode of failure to the fracture of the strip it self and avoids the fracture of the anchorage scheme.

When a properly designed anchoring device is employed the mode of failure is driven to the fracture of the FRP strip, resulting to an increase of the ultimate bearing capacity of the strengthening scheme and an increase of the exploitation of the material. The uncertainties imposed by this type of FRP anchor, such as the complete impregnation of the epoxy into the fibers of the anchor, the percentage of the fibers that are fractured during installation, the stress concentration at the edges of the anchoring scheme, are leading the writers to investigate another anchoring device made of steel components which has been patented in Europe under the patent number WO2011073696 [15]. The following paragraph deals with the numerical development of such a novel anchoring setup utilizing the numerical simulation software ABAQUS.

2.3 Numerical development of the novel patented anchoring scheme

At this preliminary design stage, the novel patented anchoring scheme was initially developed through a parametric numerical simulation, which is eventually supplemented by specific tests with pilot anchor specimens. It should be noted that the developed numerical models are rather crude since they aim to extract the basic structural response of the proposed novel anchoring scheme, which are further studied experimentally. Figure 3 depicts the main outline of the device. It consists of two vertical steel bolts that support a horizontal cylindrical steel rod. The largest portion of the vertical steel bolts below the horizontal rod has sufficient length and shape to be effectively embedded within the volume of the R/C foundation. The horizontal steel rod is utilized to facilitate the wrapping of FRP layers around it. Both wings of these FRP layers wrapped around the steel rod become one sheet that is next attached, with the use of epoxy resin and anchor bolts, on to the side of the R/C pier specimen to a sufficient length.

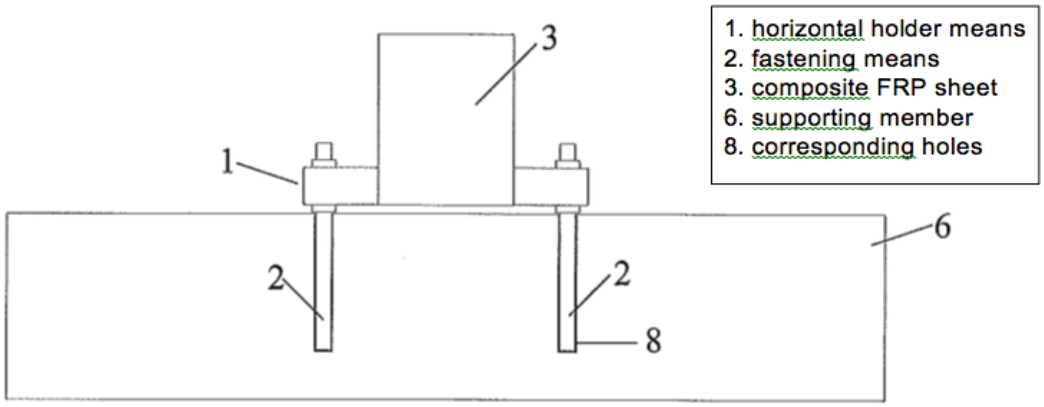

Figure 3. Novel patented anchoring device (WO2011073696 [15])

The limit state that concerns the debonding of FRP layers from the side of the pier specimen is experimentally controlled through this specific attachment technique and the attachment length; as a result it is not investigated further in this section. Furthermore the vertical steel bolts are assumed to have sufficient embedment details as to provide the required resistance against the limit state that leads to the pull-out of these bolts from the concrete foundation. Thus, excluding the debonding of the FRP layers from the side of the specimen and the pulling out of the embedded vertical steel bolts, the remaining failure modes that are considered in the parametric investigation are threefold. The first mode is the yielding and eventual fracture of the vertical steel bolts at the portion that lies between the foundation and the horizontal rod. Any other type of failure of the connection between the vertical bolts and the steel rod is excluded. The second mode of failure is the yielding of the steel horizontal rod and the third and last mode of failure is the fracture of the FRP sheet, which is wrapped around the horizontal rod.

A FEA commercial program, ABAQUS, is used for the parametric numerical simulation utilizing 3D finite elements. The horizontal rod is assumed to be made of mild steel with yield stress equal to 360Mpa, whereas the vertical bolts are assumed to be made of high yield point steel (550Mpa). In any case the same type of investigation can be easily repeated with alternative material properties.

Thus the parametric investigation focuses on the following specific parameters that are directly connected with the novel anchoring scheme. These are:

a) the width and thickness of the FRP layers that are wrapped around the horizontal steel rod
b) the span and the diameter of the horizontal rod
c) the length and the diameter of the portion of the vertical bolts that lies between the foundation and the horizontal rod.

All the parameters mentioned in the a), b), c) above are varied within certain practical limits in order to investigate the sensitivity of the behavior of the novel and patented anchoring scheme to their variation. Of the outmost interest is how the variation of these parameters (a,b,c above) influences the post-elastic behavior and the prevailing mode of failure.

A tri-linear constitutive material low is assumed for the mild steel and the high yield strength steel whereas the FRP layers are assumed to be made of carbon and to behave elastically till a fracture limit stress. The corresponding values for the constitutive laws of each one of these three materials, which were assigned in this particular software, are listed (Table 3).

Table 3. Material properties of the novel, patented anchoring device

Part of HAD	Modulus of Elasticity (Mpa)	Yield stress (Mpa)	Ultimate stress (Mpa)
Horizontal Steel Rod	200000	360	396
Vertical Steel Bolts	200000	550	650
CFRP Sheet	500000	-	5500

Figure 4 shows a typical geometry of the device with a horizontal rod having a total length equal to 280mm and a diameter of 40mm. The vertical steel bolts have a diameter of 18mm. As mentioned before, this is an initial geometry with certain parameters varied through the parametric numerical investigation.

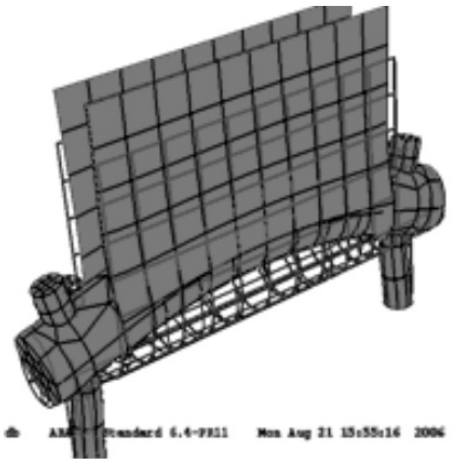

Figure 4. A typical geometry of the novel, patented anchoring device

The numerical investigation assumed, as well, that the bottom ends of the vertical steel bolts are fully fixed. Moreover, the connection between the horizontal rod and the vertical steel bolts was assumed to be monolithic. The loading was imposed as a prescribed uniform vertical displacement pattern at the full length of the upper part of the CFRP sheet. As a result, the CFRP is subjected to tension whereas the horizontal rod undergoes flexure. The contact surface between the CFRP sheet and the horizontal rod is considered as frictionless; thus the CFRP sheet can slip or move independently from the rod.

A large number of parametric numerical simulations have been conducted. Tables 4 and 5 present the most important numerical models that were employed to study the novel, patented anchor's behavior. They are categorized according to the investigated variable, which is listed in the rows of the first column. For the numerical simulations that correspond to each one of the main rows of Tables 4 and 5, the values of the corresponding variable are changed as listed, whereas the values of all the other parameters remain constant (with italics in the 1st column of Table 4) as defined in the initial geometry; that is a horizontal rod with a length of 280mm (235mm from the supports), and a CFRP layer of thickness 0.7mm (4 layers) with a length of 180mm. The typical geometry of the vertical steel bolts is of 18mm diameter and 70mm length. A typical deformed shape of the numerical model of the anchor under the imposed displacement pattern is depicted in Figure 4.

In the first row of Table 4 the variable parameter is the diameter of the horizontal rod from 40mm to 20mm. Figures 5a, b, c depict the axial stress distribution for the CFRP sheet wrapped around the horizontal steel rod. As expected, the bigger the diameter of the horizontal rod the smaller the curvatures it develops along its axis leading to a more uniform axial stress distribution for the CFRP sheet, as shown by the white line diagram that represents the axial stress distribution on a cross section 40mm from the axis of the rod. It was assumed that a strain of 1.1% resulted in the failure of the CFRP sheet.

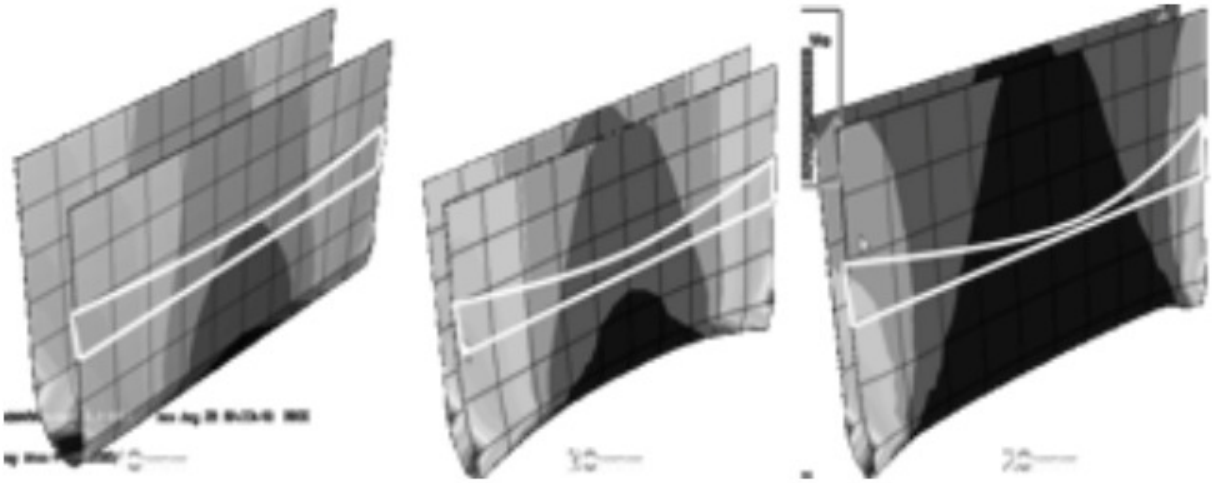

Figure 5. Distribution of axial membrane stresses

Table 4. HAD with uniform diameter of the horizontal steel rod

Studied variable	Value of variable parameter	Applied Total Axial Load (kN)	No. CFRP layer	Limit Displacement (mm) Leading to failure	Mode of failure
(1)	(2)	(3)	(4)	(5)	(6)
rod's diameter *(rod's span 280mm) (CFRP's width 200mm)*	40mm	168	4	1.2	CFRP rupture
	30mm	119	4	1.0	CFRP rupture
	20mm	55	4	0.87	CFRP rupture
rod's span / CFRP's width *(rod's diameter 40mm)*	380mm / 200mm	131	4	2.5	CFRP rupture
	380mm / 300mm	180	4	1.5	CFRP rupture
	200mm / 120mm	217	4	2.5	CFRP rupture
rod's diameter *(rod's span 280mm) (CFRP's width 200mm)*	40mm / 30mm / 20mm	622 / 368 / 158	15 / 9 / 5	30 / 20 / 20	Rod yielding

In the second row of Table 4 the variable parameters is the ratio of the CFRP sheet width over the length of the horizontal steel rod. As can be seen, when this ratio is increased from an initial value corresponding to the typical geometry, this leads to a less uniform axial stress distribution and consequently to a relatively premature fracture of the CFRP sheet. This is again due to the fact that a relatively flexible rod develops larger curvatures along its axis thus influencing the corresponding axial stress distribution of the CFRP sheet. From the above observations it can be further concluded that it is not desirable to have a steel rod, either of relatively small diameter or large span, which develops large curvatures at the part where the CFRP sheet is wrapped around it. At the same time, horizontal rods with relatively large diameter and small span perform in elastic state of stress leading the HAD to develop either fracture of the CFRP, which also remains almost elastic up to its fracture, or leading to the yielding of the vertical steel bolts; the latter present a possible plastic mode of failure as will be discussed next. The resulting non-uniform distribution of the axial stress for the CFRP sheet for relatively large curvatures of the horizontal rod was accompanied by a decrease in the bearing capacity of the device in terms of limit imposed displacement (column 6 of Table 4) and applied total axial load (column 3 Table 4).

At this point it should be mentioned that for the current investigation the longitudinal shear strains were relatively small ($\approx 1.2 \cdot 10^{-4}$), which led to the adoption of a rather simplified failure criterion based on the longitudinal strains. For other more complex applications a more sophisticated failure criterion could be included in the future, which will not neglect the possibility of shear splitting failure.

In the third row of Table 4, the thickness of the CFRP sheet was increased to 2.63mm (15 layers) in order to lead the novel anchoring device into the yielding mode of the horizontal steel rod. As was expected, the smaller diameter rod resulted in much smaller yielding load of the device; however, in all these cases with the yielding of the horizontal rod, the limit total axial load (column 3 of Table 4) attained values larger than the corresponding values for all the previously investigated cases (rows 1 and 2) where the mode of failure developed due to the fracture of the CFRP sheet. Moreover, the obtained load-displacement behaviour of the patented anchoring scheme with the yielding rod, exhibited post-elastic trends that represent a desirable feature of its performance. Consequently, from all these findings of the numerical investigation it became obvious that the numerical performance of the device with a variable diameter, as shown in Figure 6, should be examined next.

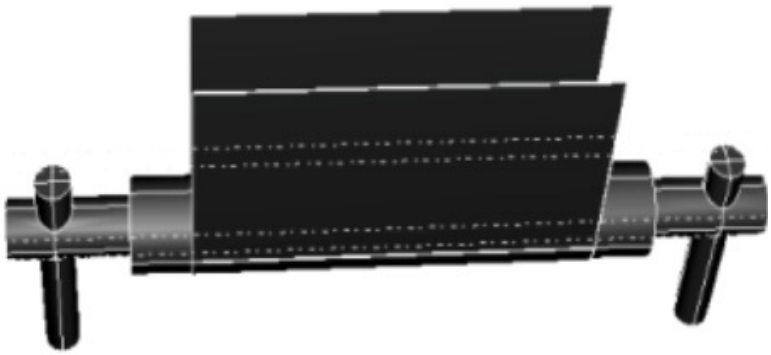

Figure 6. Patented anchoring device with variable diameter

Table 5. HAD with variable diameter of the horizontal steel rod

Studied variable	Value	Applied Load (kN)	No. CFRP layer	Limit Displ. Leading to failure (mm)	Mode of failure
(1)	(2)	(3)	(4)	(5)	(6)
rod with variable diameter	Max diameter: 40mm (span 200mm) Small diameter:20mm (40mm each side)	180.5	4	5.7	Plastic region yielding
Vertical bolt diameter @ length	18mm @ 100mm / 18mm @ 70mm	278 / 300	6 / 6	12 / 10	Vertical Bolt yielding
	20mm @ 100mm / 20mm @ 70mm	310 / 340	6 / 6	10 / 7.5	
Tested HAD	D_{rod} = 40mm L_{rod} = 340 mm L_{CFRP} = 120 mm	48	4	2.35	CFRP rupture

This novel anchoring device model had a horizontal rod with two specific regions; the region near the vertical steel bolts was made with a diameter smaller than the diameter of the central region. The values of these parameters are listed in the first row of Table 5. The reduction of the diameter of the horizontal rod was aimed at developing the large curvatures from flexure leading to the yielding of these two regions, whereas the central region with the relatively large diameter, used for the wrapping of the CFRP sheet, developed much smaller curvatures and thus prohibited the premature fracture of the CFRP. In Figure 7 the obtained load-displacement behavior of the patented scheme with variable diameter is compared with the corresponding behaviour of two model device's with constant diameter. There is no plasticification of the steel rod for the first model with constant diameter value the same as that of the central region of the variable-diameter-scheme (large diameter). On the contrary, plasticification of the steel rod is evident for the second model with constant diameter value equal to the small diameter of the variable-diameter. Similar plasticification is evident for the variable di-

ameter patented device, which develops the desired performance in terms of ductile behavior. Moreover, because of the non-plastification of the central region, which is accompanied with relatively small curvatures, the undesirable premature fracture of the CFRP is avoided.

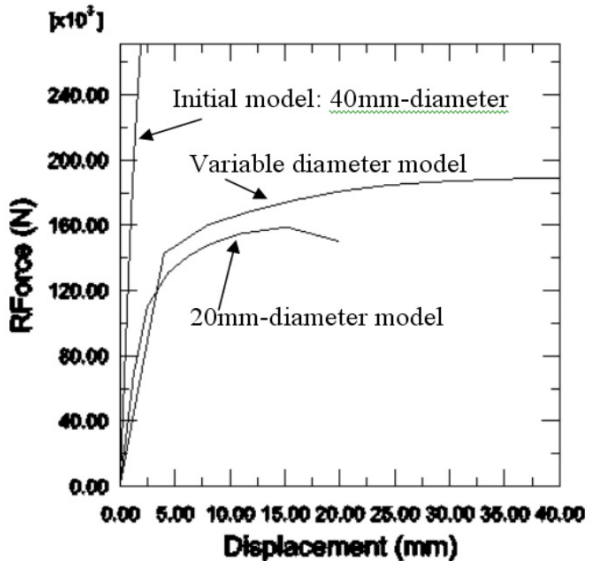

Figure 7. Load-Deflection diagram for the three models

The parameters that are varied in the second row of Table 5 are the diameter and length of the vertical steel bolts. In the corresponding numerical simulations the thickness of the CFRP sheet was increased to 1.05mm (6 layers) in order to lead the HAD into the yielding mode of the vertical steel bolts. The diameter of these bolts was varied from18mm to 20mm whereas the clear length was varied from 70mm to 100mm. In the initial modeling of the yielding behavior of the vertical steel bolts, the horizontal rod was artificially assumed to remain elastic. After this behavior was verified the next numerical model of the variable-diameter model was purposely formed to be capable of capturing the yielding mode of failure either of the vertical steel bolts or of the small diameter portion of the horizontal rod. As expected, relatively small-diameter, long vertical bolts will eventually lead the yielding mode of failure to these bolts rather than the horizontal rod, if so desired. As a result, varying the basic parameters of the device, e.g. the small diameter of the rod, the diameter of the vertical bolt and the number of CFRP layers (with their width and thickness), the desired performance of the patented device in terms of ductile bearing capacity and mode of failure can be obtained by the proposed numerical investigation as a preliminary design of this novel patented anchoring scheme. From the preceding investigation, the ductile performance can be obtained by either the yielding of the small diameter portion of the rod or by the yielding of the vertical bolts, or if the parameters are adjusted properly by the yielding of both parts. However, it is believed that the yielding of the small diameter portion of the horizontal steel rod is preferable as the device can be manufactured in such a way that the ductile behavior of this part is reversible. It is believed that the vertical bolts should have a capacity large enough (with sufficient embedment within the concrete foundation) to exclude the possibility of any pull-out failure mode. Finally, the deformed horizontal rod can be replaced more easily compared to the replacement of the vertical bolts.

The last row of Table 5 lists the parameters of a final numerical model, which was eventually manufactured and tested experimentally as will be explained in the following.

This final numerical device model, depicted in Figure 8, had a horizontal rod with two specific regions called regions of plastic hinges, which were of a diameter smaller than the di-

ameter of the horizontal rod away from these regions. This numerical model incorporated all the capabilities of the previously performed investigation in terms of non-linear behavior. Thus, the rod had sufficient diameter at both of its edges as to be able to incorporate relatively large diameter vertical bolts and confine the yielding of the device at specific regions named "plastic hinges". This final numerical model, with the two plastic hinge regions, developed, as expected, a more uniform distribution of the axial tensile stresses for the CFRP without significant stress concentration that may potentially lead to premature tensile fracture of the CFRP unlike the model with constant diameter. Finally, considerable plastic strains developed at the plastic hinges thus providing this model with the desired ductile behavior for a target axial load bearing capacity (Figure 9).

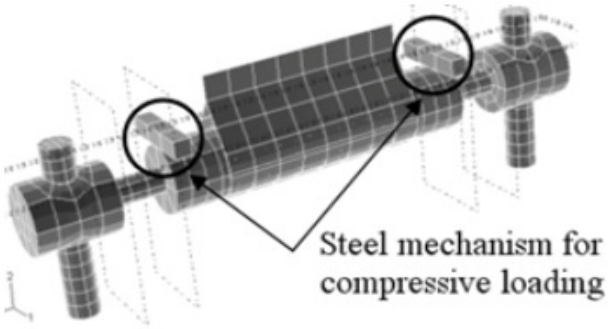

Figure 8. Novel patented anchoring scheme model with plastic hinges (zones)

3 EXPERIMENTAL INVESTIGATION OF THE NOVEL DUCTILE ANCHORING DEVICE UNDER LOAD-UNLOAD SEQUENCE – NUMERICAL VALIDATION

3.1 Experimental setup – cyclic loading sequence

Different anchoring schemes of FRP strips, under monotonic loading conditions, have been studied in the past by several researchers. [12-19] On the other hand experimental investigations under cyclic loading – unloading sequence are rare in the literature. The present study is moreover, focusing on experimentally investigating under cyclic loading conditions, the novel anchoring device developed by the Laboratory of Strength of Materials and Structures of Aristotle University of Thessaloniki in Greece, which is patented with patent number EP 09386037.7 [8,15].

Totally 3 specimens were tested under cyclic loading – unloading conditions. The idea of investigating experimentally the novel and patented anchoring scheme with combining FRP strips is further examined in this section. There are small differences in the shapes of the anchoring device in order to investigate the developed ductility on the anchoring scheme. The first type is an anchoring scheme with plastic zones. The second type is identical with the first type with a small change, which is located in the plastic zones that have smoother corners. Finally the third type is an anchor device without any plastic zone. Figures 9a to 9c present the different types of the novel anchoring device.

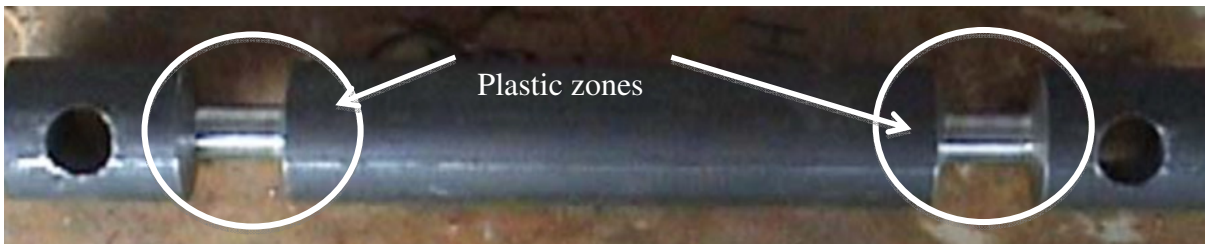

Figure 9a. First type of anchoring scheme

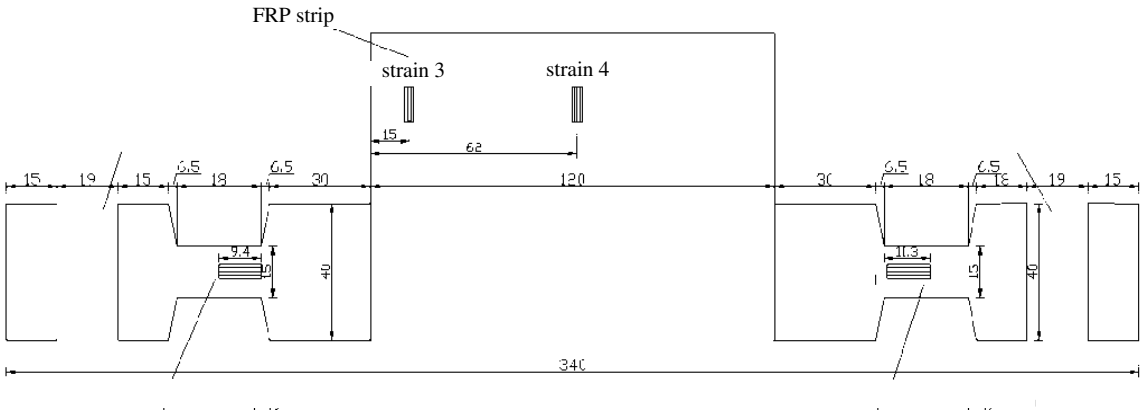

Figure 9b. Second type of anchoring scheme

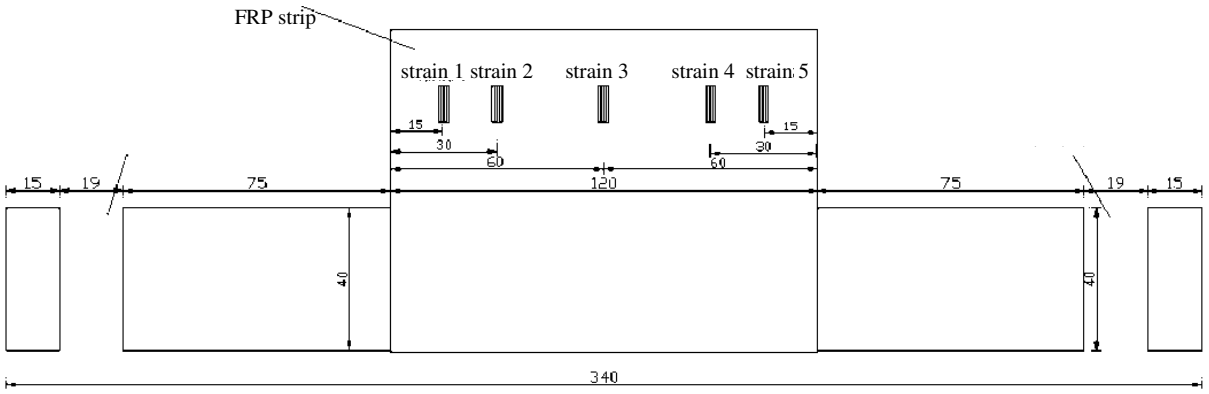

Figure 9c. Third type of anchoring scheme

The experimental setup is depicted in the following figures 10a and 10b. The cyclic loading unloading displacement is imposed utilizing a hydraulic actuator. The imposed load is monitored with a 100kN dynamic load cell.

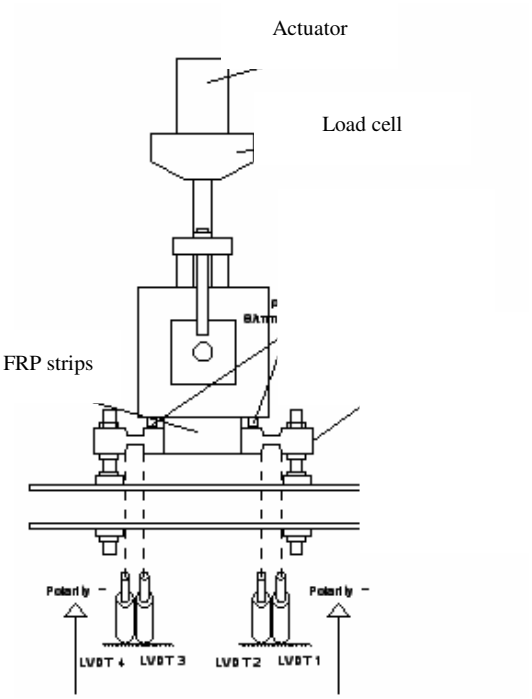

Figures 10a and 10b. Experimental setup and instrumentation

At the same time four LVDTs are place at the edges of the plastic zones (see figure 11) to monitor their relevant deformations. Finally strain gages were placed to several positions in order to measure accurately the developed strains and stresses both on the anchoring device and on the FRP strips.

The imposed displacement protocol is depicted in the following figure 12. The target displacement was imposed for three cycles and was increased up to failure. For the first and second type of the anchoring scheme, a metallic prismatic element was utilized to enable the ability of the anchoring scheme to withstand negative forces during the unloading sequence.

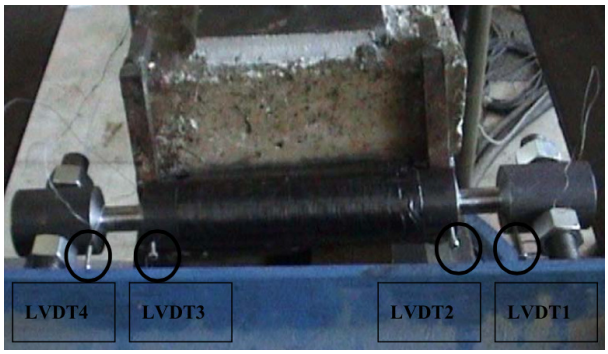

Figure 11. Position of LVDTs at plastic zones

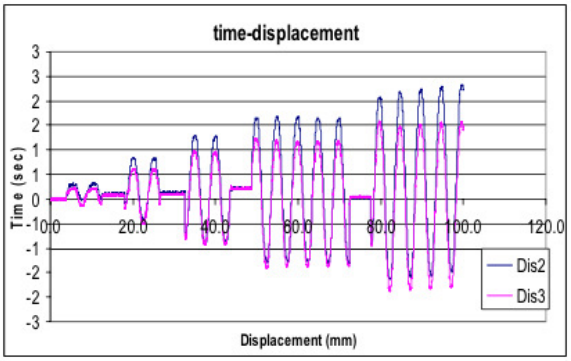

Figure 12. Imposed displacement protocol

3.2 Experimental results – cyclic loading sequence

The cyclic loading – unloading sequence was performed to all three types of the novel patented anchoring scheme that is combined with FRP strips. Figures 13a to 13e present the load - displacement graphs for the three types of the anchoring scheme.

Table 3. Load – displacement graphs for the three types of the novel anchoring scheme

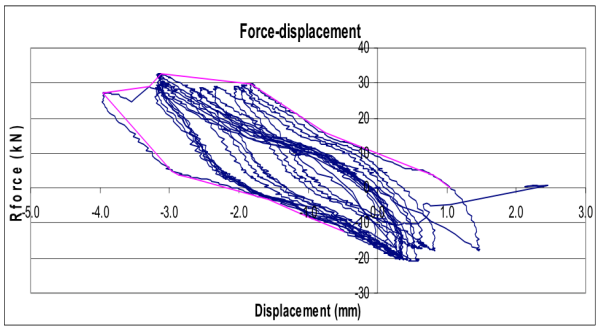

Figure13a.Total force – Displacement of type_1 anchor

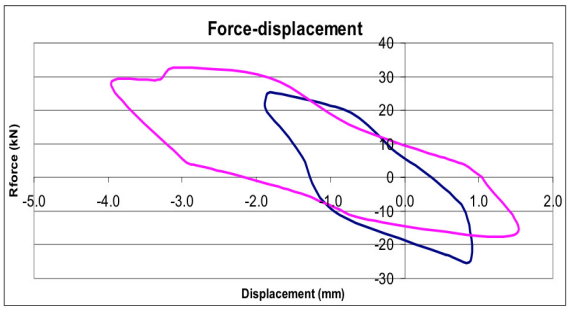

Figure13b. Envelope curves of type_1 anchor

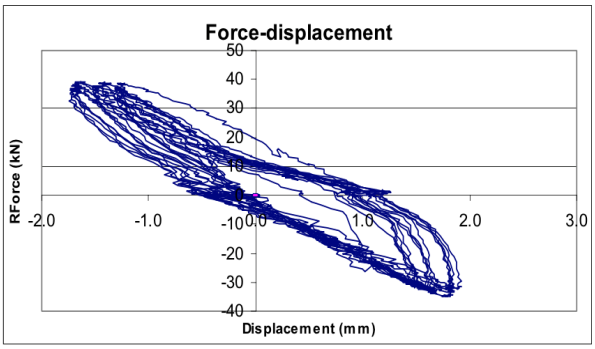

Figure13c.Total force – Displacement of type_2 anchor

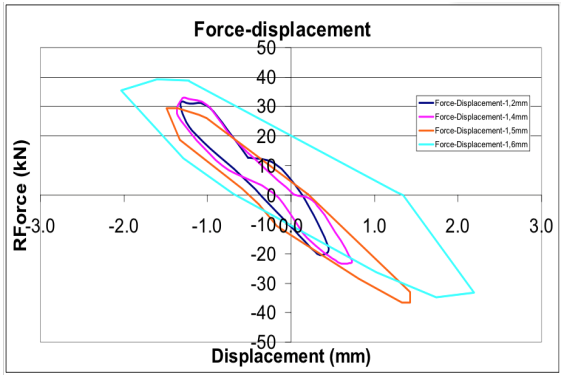

Figure13d. Envelope curves of type_2 anchor

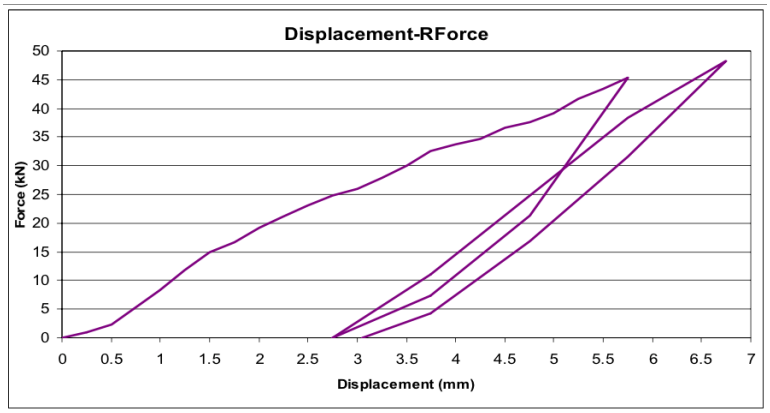

Figure13e. Total force – Displacement of type_3 anchor (two cycles of loading – unloading)

Taking under consideration the graphs depicted above, it could be said that the overall behavior of the strengthening system FRP strip – Anchoring device exhibit a relative ductile behavior. Anchoring schemes with plastic zones exhibit a more ductile behavior than the anchoring zone without the plastic zone (3rd type). The number of cycles does not affect significantly the behavior of the strengthening system. The potential influence of the number of

cycles could arise because of the type of the material, since the components of the anchoring device are made of steel. This parameter is not investigated in the present study.

The novel anchoring device for FRP strips was tested under cyclic loading – unloading sequence. All three types of the novel anchoring device behaved in-elastically. The use of the anchoring system results in transmitting the linear developed stresses of the FRP strip, to the concrete elements in a ductile manner through this patented anchoring device. It is obvious that when the plastic zones exist, the ductile behavior is more pronounced.

The following figure 14 presents four load-stress graphs. The blue and brown curves depict the strains in the middle and at the corner of the width of the FRP strip that is wrapped around the anchoring device with the plastic zones. The yellow and pink curves present the equivalent strains on the FRP strip when it is combined with the anchoring device without the plastic zones.

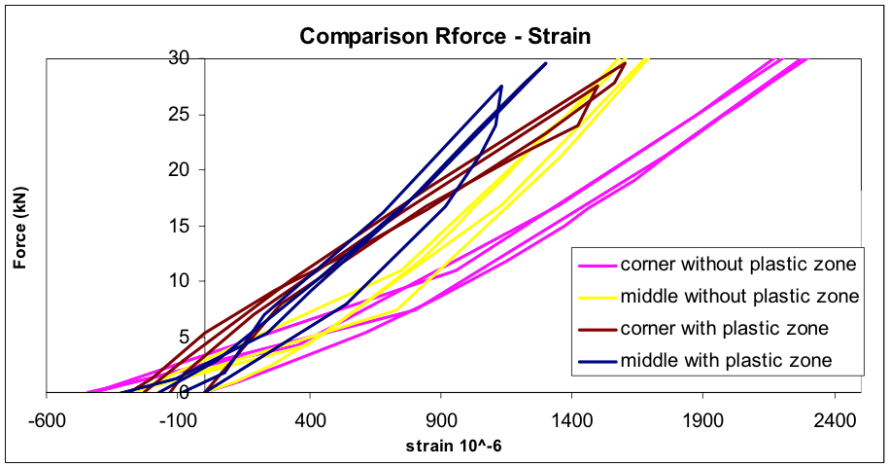

Figure 14. Comparison total load – developed strain graph with and without plastic zones

Table 6. Modes of failure for all three types of the novel anchoring device

Yielding and fracture of plastic zone (type_1 anchor)

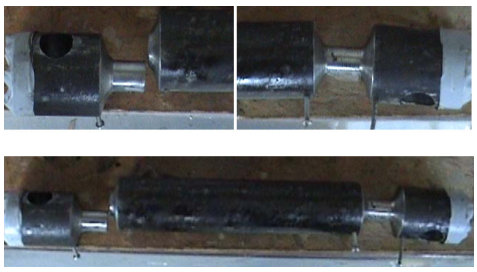

Yielding and fracture of plastic zone (type_2 anchor)

Fracture of FRP strip (type_3 anchor)

It is evident that the stress distribution on the FRP strip with the plastic zones is more uni-

form than the equivalent one without the plastic zones. In this point of view and based on the results of the monotonic loading sequence, when the novel anchoring device has the plastic zones, the FRP strip could be exploited more efficiently.

The modes of failure are depicted in table 6. The yielding of plastic zones was followed by their fracture. On the other hand type 3 anchoring scheme, without plastic zones, drove the mode of failure to the fracture of the FRP strip, a much less ductile mode of failure.

3.3 Numerical validation – cyclic loading sequence

The experimental behavior of the novel, patented anchoring scheme is compared with the numerical results of the aforementioned investigation. The mechanical properties of the materials forming the pilot device specimens were obtained by specific tensile experiments that resulted in mechanical values the same as the ones used in the numerical simulation. One pilot novel anchoring device specimen was made with a horizontal steel rod of constant diameter whereas the other had a variable diameter with the aforementioned plastic hinge zones at specific locations, as shown in Figure 8.

Apart from this difference all the rest of the geometric and material properties were the same for all specimens. The depicted geometry is the same as the one assumed as being "typical" for the performed parametric numerical investigation; that is, a horizontal rod with a length of 340mm (290mm from the supports), an initial diameter of 40mm (and a diameter at the plastic hinge regions of 15mm) and a CFRP layer of thickness 0,7mm (formed by 4 CFRP layers) with a length of 120mm. Each plastic hinge region had a length of 20mm and each vertical steel bolt was of 18mm diameter and 70mm length. These two pilot novel anchoring specimens, including the CFRP layers wrapped around their horizontal steel rod, were placed in a reaction frame, which included a dynamic actuator (Figure 10), as mentioned before.

The strains measured at the CFRP sheets are compared with the values predicted from the corresponding numerical simulation. Next, to compare the measured overall load-displacement response of the pilot HAD specimens with that predicted numerically. Finally, to compare the observed mode of failure for both pilot HAD specimens with the relevant limit states predicted by the numerical simulation.

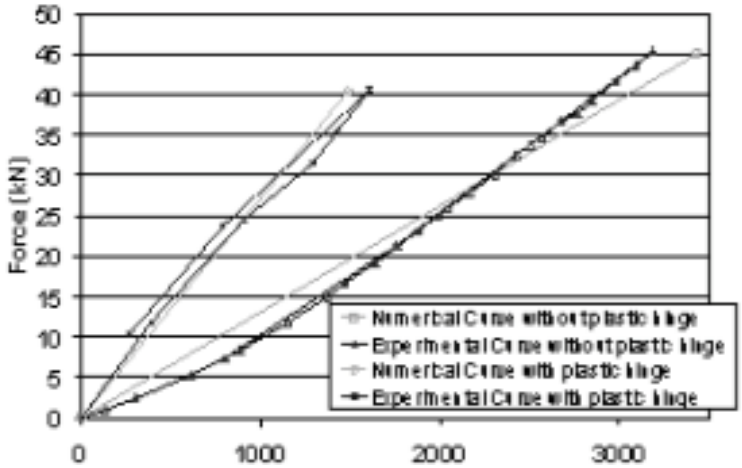

Figure 15. Numerical vs Experimental load-strain variation for the novel anchoring scheme with and without plastic zones (CFRP strains at edge of the CFRP layers)

The term axial strain indicates that the axis of the strains measured by the strain gauges coincide with the axis of the applied load and the axis of the carbon fibers forming the CFRP strips. The variation of the predicted and measured axial strains against the applied load are plotted in Figure 15. This is done for all novel, patented anchoribg schemes with or without plastic zones. For given amplitude of applied load the strains measured near the edge of the CFRP sheet are considerably larger than the corresponding strains measured at the middle of this CFRP sheet, validating a similar finding of the numerical investigation (Figures 5 and 14). As has been already pointed out, this is an undesirable state of stress, which can lead to premature tensile failure of the CFRP sheets. In contrast, the measured strains at the CFRP wrapped around the horizontal rod of the variable-diameter-HAD with the plastic hinge regions remain almost constant along the width of this CFRP sheet, a fact that also verifies the numerical investigation findings. On the basis of this evidence, it can be concluded that the proper location of the "plastic zone" regions along the span of the horizontal rod of the novel anchoring scheme, results in the mitigation of an undesirable non-uniform tensile stress field for the wrapped around this rod CFRP strips.

Figure 16 depicts the measured and numerically predicted applied load – displacement response for the device specimen with the plastic hinges. As can be seen in this figure, the predicted load level that corresponds to the development of large deformations (due to the material yielding of the plastic regions) agrees well with the corresponding measured value.

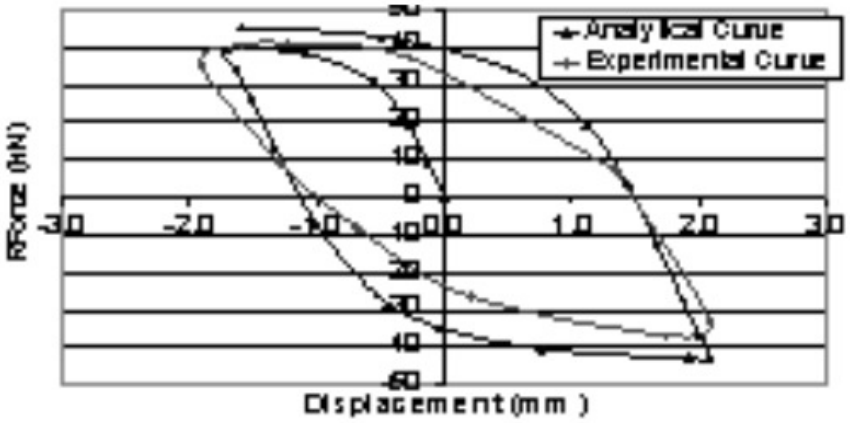

Figure 16. Load-deflection numerical and experimental behavior

The measured initial stiffness is smaller than the numerically predicted value, a fact that must be attributed to the deformability of the vertical steel bolts connecting the experimental anchoring scheme specimen to the reaction frame. This observation can also be made when comparing the predicted and measured load-deflection response of the scheme without the plastic hinge regions. For an applied load of 40.4 kN the measured strain values are compared with the corresponding numerical strains for both the CFRP sheet (left part of Figure 17) and the plastic hinge zone of the horizontal rod of the variable-diameter anchor specimen (right part of Figure 17, $\varepsilon = 1.13\%$). Reasonably good agreement can be seen in this comparison.

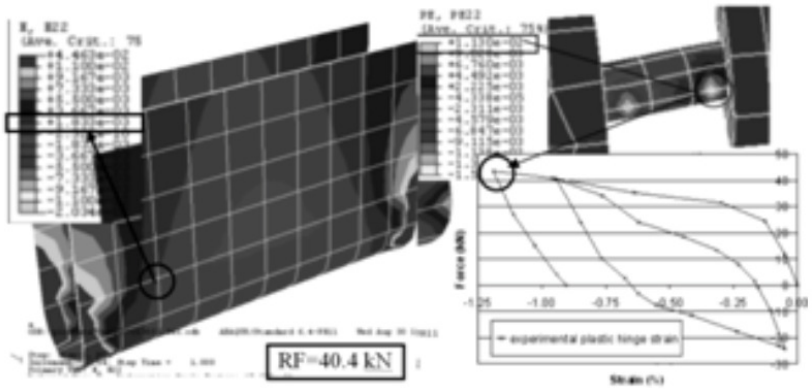

Figure 17. Developed strains on CFRP and on plastic zone

Finally, as discussed in the previous section, the brittle fracture of the CFRP sheet occurred, as expected, for the novel patented anchoring scheme without the plastic hinge zones. In contrast, the patented anchoring scheme with the plastic zones exhibited, as predicted, reasonably good ductile behavior, due to the yielding of the steel at the plastic zones; this led eventually to the fracture of the left plastic hinge, after a considerable number of load reversals that exceeded the measuring capacity of the strain gauges (Table 6). On the basis of all these observations it can be concluded that the behavior of the novel, patented anchoring device can be predicted numerically with sufficient accuracy employing the previously prescribed modeling procedure.

4 CONCLUSIONS

- In order to transfer effectively the tensile forces developed on FRP strips that are bonded externally towards upgrading the flexural or shear capacity of reinforced concrete members a properly designed anchoring device should be employed. In this way, the premature FRP strip debonding mode of failure can be prohibited and instead direct the mode of failure to either the fracture of the FRP strip or the yielding of the anchoring scheme, thus resulting in a substantial increase of the ultimate bearing capacity of the strengthening scheme.
- Such an anchoring device, designated as SWFX, was examined in the framework of the present study under monotonic load conditions. It utilizes one or two FRP anchors with one CFRP strip. This anchoring scheme ensures up to a certain level of load the safe transfer of forces from the strip to the R/C prism. However, the final mode of failure is the fracture of the FRP anchor.
- The alternative patented anchoring device, which is designated as anchoring device with European Patent, utilizes two steel anchor bolts and a steel rod. When properly designed it can withstand one or more FRP strips with the final mode of failure directed either to the fracture of the FRP strips or to the plastic zones of the device itself. In this way a very substantial increase of the targeted bearing capacity could be reached. Moreover, an effective exploitation of the FRP material can also be achieved.

- The anchoring device with the EU patent can also be detailed in a way that can include a zone that can be plastified at certain level of force to be transferred. The stress distribution on FRP strip with such plastic zones is more uniform than the equivalent one without the plastic zones. In this way the FRP strip is protected from premature fracture, which is a common undesired mode of failure that occurs in such FRP location of stress concentration.
- Such an anchoring device with plastification zones was examined under cyclic seismic-type loading. It is demonstrated that this anchoring device was able to withstand a considerable number of cyclic load reversals performing in a stable way and dissipating plastic energy through the zones of the steel rod that this anchoring device was detailed for.
- As already stressed, it is of the utmost importance the design and the detailing of such an effective anchoring device. Towards this objective, results from series of numerical simulations were compared with the corresponding experimental measurements in order to establish the validity of such a numerical simulation as a design tool for such an effective anchoring device.

5 ACKNOWLEDGEMENTS

- Carbon fibers, anchors and epoxy resins were provided by Sika Hellas.
- One of the employed in this study anchoring devices (cyclic investigation) is patented under the no. EP09386037.7
- PartialfinancialsupportforthisinvestigationwasprovidedbytheHellenicEarthquakePlanning and Protection Organization (EPPO)

REFERENCES

[1] C. E. Bakis, L. C. Bank, V. L. Brown, E. Cosenza, J. F. Davalos, J. J. Lesko, A. Machida, S. H. Rizkalla, T. C. Triantafillou. In: Journal of Composites of Construction, ASCE, May 2002.

[2] Manos G.C., Theofanous M., Katakalos K. “Numerical simulation of the shear behaviour of reinforced concrete rectangular beam specimens with or without FRP-strip shear reinforcement”, Advances in Engineering Software, 2014Mich. Fardis, M. N., and Khalili, H. ~1981in: ACI J., 78~6, 440–446.

[3] K Katakalos, CG Papakonstantinou, “Fatigue of reinforced concrete beams strengthened with steel-reinforced inorganic polymers”, Journal of Composites for Construction 13 (2), 103-112C.

[4] CG Papakonstantinou, K Katakalos, “Flexural behavior of reinforced concrete beams strengthened with a hybrid inorganic matrix-Steel fiber retrofit system”, Structural Engineering and Mechanics 31 (5), 567-585

[5] GC Manos, K Katakalos, CG Papakonstantinou, “Shear behavior of rectangular beams strengthened with either carbon or steel fiber reinforced polymers”, Applied Mechanics and Materials 82, 571-576

[6] J. H. Lee, M. M. Lopez, C. E. Bakis. “Flexural Behavior of reinforced concrete beams

strengthened with mechanically fastened FRP strip." FRPRCS-8, World Conference, University of Patras, July, 2007.

[7] GC Manos, K Katakalos, V Kourtides, "The influence of concrete surface preparation when fiber reinforced polymers with different anchoring devices are being applied for strengthening R/C structural members", Applied Mechanics and Materials 82, 600-605

[8] GC Manos, KV Katakalos, "The Use of Fiber Reinforced Plastic for The Repair and Strengthening of Existing Reinforced Concrete Structural Elements Damaged by Earthquakes", Fiber Reinforced Polymers - The Technology Applied for Concrete Repair

[9] Katakalos K, Papakonstantinou CG, Manos GC. Comparison between carbon and steel fiber reinforced polymer with or without anchorage. In: 6th CICE, Rome; 2012. □

[10] Lu XZ, Teng JG, Yea LP, Jiang JJ. Bond–slip models for FRP sheets/plates bonded to concrete. Eng Struct 2005;27:920–37. □

[11] Manos GC, Katakalos KV, "The Use of Fiber Reinforced Plastic for The Repair and Strengthening of Existing Reinforced Concrete Structural Elements Damaged by Earthquakes", Chapter 3, Fiber Reinforced Polymers - The Technology Applied for Concrete Repair

[12] Manos GC, Katakalos KB, Theofanous M., "Experimental Investigation and Numerical Simulation of Shear Behaviour of RC T-Beam Specimens with or without SFRP-strips under Cyclic Loading", Computational Dynamics, Conference, Krete-Greece, 2015

[13] Manos GC, Katakalos, KV "Investigation of the Force Transfer Mechanisms for Open Hoop FRP Strips Bonded on R/C Beams with or without Anchoring Devices", Open Journal of Civil Engineering, 143-153

[14] Manos GC, Katakalos K., "Enhanced Repair and Strengthening of Reinforced Concrete Beams Utilizing External Fiber Reinforced Polymer Sheets and Novel Anchoring Devices", 15th World Conference of Earthquake Engineering

[15] Manos GC, Katakalos K, Kourtides V. Construction structure with strengthening device and method. European Patent Office, Patent Number WO2011073696 (A1); 2011 (23.06.11). □

[16] Manos GC, Katakalos K, Kourtides V. Cyclic behaviour of a hybrid anchoring device enhancing the flexural capacity and ductility of an R/C bridge-type pier strengthened with CFRP sheets. J Civ Eng Res 2012.

[17] Manos GC, Katakalos K. The use of fiber reinforced plastic for the repair and strengthening of existing reinforced concrete structural elements damaged by earthquakes. In: Masuelli Martin Alberto, editor. Published in the book, Fiber Reinforced Polymers – The Technology Applied for Concrete Repair; January 23, 2013, ISBN: 978-953-51-0938-9 [ch.3]

[18] Paz, Mario. International handbook of earthquake engineering: codes, programs and examples. In: Greece by G.C. Manos, editor. Chapman and Hall; 1994. [chapter 17].

[19] Wu Y, Zhou Z, Yang Q, Chen W. On shear bond strength of FRP-concrete structures. Eng Struct 2010;32:897–905.